

# PAPR reduction scheme: wavelet packet-based PTS with embedded side information data scheme

ISSN 1751-8628

Received on 28th January 2016

Revised on 9th September 2016

Accepted on 16th September 2016

doi: 10.1049/iet-com.2016.0101

www.ietdl.org

Jamaluddin Zakaria, Mohd Fadzli Mohd Salleh ✉

School of Electrical and Electronic Engineering, Universiti Sains Malaysia, Seri Ampangan, 14300 Nibong Tebal, Pulau Pinang, Malaysia  
 ✉ E-mail: fadzlisalleh@usm.my

**Abstract:** Partial transmit sequence (PTS) is an effective scheme to reduce high peak-to-average power ratio (PAPR) for multicarrier modulation (MCM) signal transmission systems. This approach produces side information (SI) data as a result of the MCM signal optimisation process. The generated SI data are required to be transmitted with the original data over the channel for successful data recovery at the receiver. An effective method for SI data transmission has not yet been identified and research is still ongoing. Hence, the authors introduce a technique that embeds SI data into the original data frame. In this study, a wavelet packet (WP)-based PTS (WP-PTS) scheme is selected as the MCM transmission method. The proposed scheme is called WP-PTS with embedded SI data. In addition, a suitable scheme for reconstructing the original data is developed. Simulation result shows that the PAPR performance of the proposed scheme improves by up to 2.5 dB at a complementary cumulative distribution function level of  $10^{-4}$  compared with the original WP-orthogonal frequency-division multiplexing system without the PAPR reduction scheme when the number of selected disjoint subblocks is 16.

## 1 Introduction

In recent years, research in wavelet packet-based orthogonal frequency-division multiplexing (WP-OFDM) systems has attracted numerous scholars. Implementing wavelet packet transform (WPT) instead of fast Fourier transform (FFT) in OFDM systems improves several issues.

- (i) Additional beneficial attributes to signal property, known as inherent flexibility, which provides improved spectral efficiency when the orthogonal structure is found in both the time and frequency domains of the signals [1, 2].
- (ii) The cyclic prefix (CP) becomes unnecessary in WP-OFDM systems for intersymbol interference and intercarrier interference protection while maintaining bit error rate (BER) performance [3, 4].

However, WP-OFDM transmitted signals also suffer from high peak-to-average power ratio (PAPR) because of the abundant supply of narrowband signals that accumulate in the time domain [5]. In general, a high PAPR event causes non-linear distortion of signals and reduces the power efficiency of a high-power amplifier (HPA). The use of an HPA transmitter with a wide linear region will lead to a considerable cost and increase overall system complexity; hence, PAPR reduction is a good alternative. Several excellent techniques have been proposed to diminish PAPR, including selected mapping using wavelet packet (WP) tree pruning [6], fast adaptive optimal basis search algorithm [7], combined iterative clipping and filtering methods with Huffman coding [8], and genetic algorithms [9, 10].

Among recent well-known PAPR reduction techniques based on WP-OFDM systems, the partial transmit sequence (PTS) technique is an attractive scheme because it can reduce PAPR without distorting signal orthogonality. In [11], a PTS scheme for a special multicarrier modulation (MCM) system, known as WP division multiplexing, was proposed using Daubechies 5 wavelet  $db5$ . Another work [12] proposed a method based on pruning the full-tree structure of WP modulation with the PTS scheme to reduce the number of nodes. Several works associated with low-density parity-check (LDPC) codeword were performed in

[13, 14]. The authors developed a specific parity-check matrix for the concatenated LDPC-PTS code, and PTS side information (SI) or phase factor estimation were not required before decoding [13]. To improve their previous work, the authors formulated an optimisation problem to enhance joint decoding performance by optimising partition [14].

In the conventional PTS (C-PTS) scheme based on discrete Fourier transform (DFT), input symbols are divided into  $V$  disjoint subblocks. Each subblock is phase rotated using a particular phase factor during the optimisation process. The phase factor is the SI of the appointed frame and sent along with the main information. The receiver must obtain the uncorrupted SI to realise successful data recovery [15, 16].

A highly critical issue in common PTS schemes is the manner in which they handle SI to achieve successful data recovery. We review the most effective methods proposed in the literature and classify them into two categories as follows:

- (i) Non-explicit SI approach. In [17], the research focused on generating OFDM frames in the time domain using a method called phase recursive cyclic (PRC) shifting. This method detects and recovers original signals by using the natural diversity of phase constellation. Kim *et al.* [18] proposed that an additional pilot symbol should be inserted deliberately into each subblock end of the OFDM frames. A symbol can be decoded based on channel estimation at the receiver. In [19], the authors suggested using a hard-decision maximum likelihood detector, a minimum mean square error estimator, or a zero-forcing estimator to demap quadrature amplitude modulation (QAM) symbols.
- (ii) Modified-constellation approach. Han *et al.* [20] proposed the use of a hexagonal constellation for PAPR mitigation. Given that a hexagonal constellation is the densest packing of spaced points in two dimensions, these two extra points can be utilised for SI elimination in the PTS scheme. Han *et al.* [20] also proved that the proposed uncoded 91-hexagonal (91-HEX) modulation was comparable with the conventional 64-QAM modulation. In [21], the authors proposed a reshaped QAM (R-QAM) constellation known as the R-PTS scheme. The mean square error between the constellations of the received data and the R-QAM difference

phase rotation factor are calculated at the receiver. Liang [22] proposed a sub-optimal PAPR improvement using the constellation extended scheme combined with the block-coded modulation technique in the C-PTS scheme. The extended constellation points of a 16-QAM modulation are arranged in symmetrical and asymmetrical structure where points and error correction capabilities play important roles in signal recovery.

However, in the first classified PTS method, i.e. the non-explicit SI approach, a drawback of additional time is necessary to detect or decode; as complexity increases, this drawback reduces effective transmission rate [23, 24]. Meanwhile, an unavoidable disadvantage in the second classified PTS method, i.e. the modified-constellation approach, is that various types of constellation extensions are implemented, thereby requiring higher transmission power under a mode with denser constellation points [25, 26].

The motivation for the practical application of this work is based on the fact that adding data to the frame, such as that in traditional inverse FFT (IFFT)/FFT OFDM systems, where 1/16 of the whole frame length of CP data are added to the frame in several cellular 802.11 standards [27], is widely accepted. In this work, additional SI data are incorporated to improve the quality of the reconstructed data at the receiver. Therefore, adding SI data is a practical procedure for WP systems.

The simulation results show the best performance of the proposed WP-PTS-embedded SI data (ESID) scheme exhibits a PAPR improvement of 2.5 dB compared with the original WP-OFDM curve at a complementary cumulative distribution function (CCDF) level of  $10^{-4}$  when the number of chosen disjoint subblocks is 16. This achievement incurs only minor degradation of BER performance compared with the proposed schemes in other renowned works.

The rest of the paper is organised as follows. Section 2 describes the WP-OFDM system and briefly introduces the C-PTS scheme. The proposed WP-PTS with an embedded SI index scheme and its reconstruction scheme are explained in Section 3. The simulation results are presented in Section 4. Finally, Section 5 concludes the study.

## 2 Background

This section presents PAPR computation and describes the fundamental structure of the C-PTS scheme and its features.

### 2.1 Peak-to-average power ratio

Consider an OFDM system with  $N$  subcarriers, an inverse DFT (IDFT) is applied to the complex-valued phase-shift keying or QAM input OFDM block  $\mathbf{X} = [X_0, X_1, \dots, X_{N-1}]^T$  with length  $N$  to generate the OFDM signal. The discrete time-domain OFDM signal is

$$x_n = \frac{1}{\sqrt{N}} \sum_{k=0}^{N-1} X_k e^{-j2\pi nk/N}, \quad n = 0, 1, \dots, N-1 \quad (1)$$

which can be also rewritten in matrix form as  $\mathbf{x} = [x_0, x_1, \dots, x_{N-1}]^T = \mathbf{F}^{-1}\mathbf{X}$ , where  $\mathbf{F}^{-1}$  is the IDFT matrix. In general, the PAPR of the OFDM signal is  $\mathbf{x}$ , which is defined as

$$\text{PAPR} = \frac{\max |x(t)|^2}{E|x(t)|^2} \quad (2)$$

where  $E[\cdot]$  denotes expectation.

### 2.2 C-PTS scheme

In the C-PTS scheme, an input data block with length  $N$  is partitioned into several disjoint subblocks. The IFFT for each

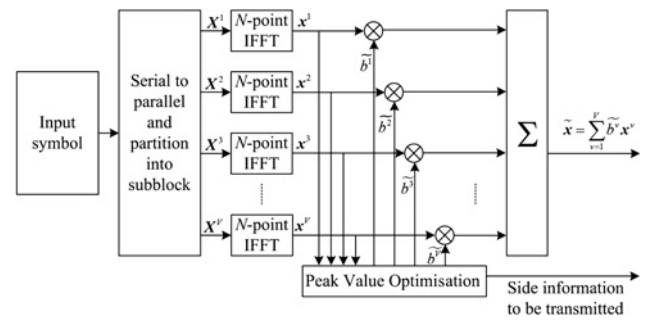


Fig. 1 C-PTS scheme

subblock is computed separately and then weighted by a phase factor. The phase factors are selected to minimise the PAPR of the combined signals of all the subblocks [28–30]. Fig. 1 shows a block diagram of the OFDM transmitter with the PTS scheme. Let an input data block,  $\mathbf{X} = [X_0, X_1, \dots, X_{N-1}]$  be partitioned into  $V$  disjoint subblocks,  $\mathbf{X} = [\mathbf{X}^1, \mathbf{X}^2, \dots, \mathbf{X}^V]$ ,  $1 \leq v \leq V$ , such that any two subblocks are orthogonal, and  $\mathbf{X}$  is the combination of all the  $V$  subblocks as

$$\mathbf{X} = \sum_{v=1}^V \mathbf{X}^v \quad (3)$$

Then, the IDFT for each subblock  $x^v$ ,  $1 \leq v \leq V$  is computed and weighted with a phase factor  $b^v = e^{j\phi_v}$ , where  $\phi_v = [0, 2\pi)$ ,  $1 \leq v \leq V$ . The objective is to select the set of phase factors  $b^v$ 's that minimises the PAPR of the combined time-domain signal  $\mathbf{x}$ , where  $\mathbf{x}$  is defined as

$$\mathbf{x} = \sum_{v=1}^V b^v \cdot \mathbf{x}^v \quad (4)$$

where

$$\mathbf{x}^v = \text{IFFT}\{\mathbf{X}^v\} \quad (5)$$

During phase factor optimisation (PFO), the search for the best phase factor,  $\tilde{b}^v$  (i.e. tilde of  $b$ ) is typically limited to a finite number of elements to reduce search complexity [5]. Assume that the set of allowed phase factors is defined as  $b^v = e^{(j2\pi k/W)}$ , where  $k = 0, 1, \dots, W-1$ , and  $W$  is the number of allowable phase factors. The first phase factor  $b^1$  is usually set to 1 without any loss in performance; therefore,  $V-1$  phase factors are found via an exhaustive search. Consequently,  $W^{V-1}$  sets of phase factors are searched to find the optimum one. The attainable reduction in PAPR depends on  $V$  and  $W$ . The larger the number of subblocks  $V$ , the greater the reduction in PAPR. However, search complexity also increases exponentially with  $V$ . In addition,  $V$  subblocks are necessary to implement the PTS scheme, which requires  $\lceil \log_2 W^{V-1} \rceil$  bits of SI for transmission [15]. The optimised transmitted signal with the lowest possible PAPR can be written as

$$\tilde{\mathbf{x}} = \sum_{v=1}^V \tilde{b}^v \cdot \mathbf{x}^v \quad (6)$$

## 3 Proposed WP-PTS-ESID scheme

This section presents the proposed WP-PTS-ESID scheme. It consists of three main parts. First, a general overview of the proposed scheme is provided, followed by the construction of the data frame. Finally, the involved algorithms are presented. To

**Table 1** Mathematical symbols used

Symbol	Description
$b$	phase factor
$\tilde{b}$	optimised phase factor
$\hat{b}$	received phase factor
$\tilde{B}$	grouped optimised phase factor
$\hat{b}$	integer factor
$\hat{b}'$	received integer factor
$v$	index number of disjoint subblocks per frame
$V$	maximum number of disjoint subblocks
$w$	number of phase factor

facilitate reading, the mathematical symbols used in this paper are listed in Table 1.

### 3.1 Overview of the WP-PTS-ESID scheme

The block diagram of the proposed WP-PTS-ESID scheme is shown in Fig. 2. An input sequence consists of the combination of two sub-sequences, i.e. dummy symbols and input symbols. This input sequence is called the data frame. The structure of the data frame is shown in Fig. 3. The SI data represent the block of the dummy symbols with length  $R$ , whereas the original data represent input symbols with length  $P$ . Therefore, a single data frame has a length of  $N$ . Initially, each dummy symbol has a value of 1 during the pre-optimisation stage. This value may change after the optimisation process. The output from the optimisation process is called the SI data.

Let the sequence of  $P$  input symbol be  $X_{data}$  and the sequence of  $R$  symbols be  $X_{SI}$ , which are regarded as a single data frame  $X_{tx}$ , where

$$X_{tx}[n] = \begin{cases} X_{SI}[n] & \text{for } 0 \leq n < R \\ X_{data}[n] & \text{for } R \leq n < N \end{cases} \quad (7)$$

where  $R = N - P$ . Then, the serial data frame  $X_{tx}$  are converted into parallel form and evenly divided into  $V$  disjoint subblocks. Let the disjoint subblock of  $X_{tx}$  along with the complex element  $b^v$  be represented as  $X$ , which is

$$X = \sum_{v=1}^V b^v \cdot X_{tx}^v \quad (8)$$

The complex element  $b^v$  is used to obtain optimised signal prior transmission. We produce the time-domain signal  $x$  obtained from the inverse discrete WPT (IDWPT) by utilising signal  $X$  as follows

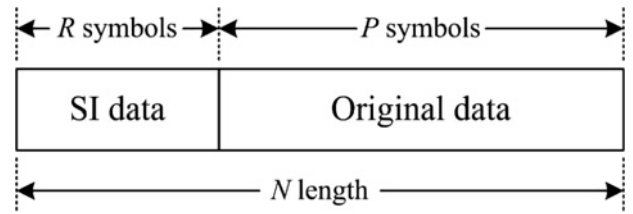


**Fig. 3** Data frame structure

$$\begin{aligned} x &= \text{IDWPT}\{X\} \\ &= \text{IDWPT}\left\{\sum_{v=1}^V b^v \cdot X_{tx}^v\right\} \end{aligned} \quad (9)$$

When the signal transform linear property is applied, (9) becomes

$$x = \sum_{v=1}^V b^v \cdot \text{IDWPT}\{X_{tx}^v\} \quad (10)$$

The term  $x$  is not shown in Fig. 2 until this point, but is used to generate the corresponding optimised phase factors known as SI data. The parameter  $b^v$  plays a key role as a signal optimiser. Hence, the  $\{b^v \cdot \text{IDWPT}\{X_{tx}^v\}\}$  term is fed into the PFO block as shown in Fig. 2. This process searches for the appropriate phase factors for subblock 1 to  $V$  that produce the lowest PAPR for the transmitted signal. To compromise with the fixed length  $R$  of the SI codeword, the length of the  $V$  sequence of the phase factors must be set to  $R$  via the process in 'b to B converter'. These two algorithmic blocks are explained in Section 3.3.

The output from the 'b to B converter' block is  $\tilde{B}$ ; that is, the SI data and (7) can be rewritten as

$$X_{tx}'[n] = \begin{cases} X_{SI}[n] = \tilde{B}[n] & \text{for } 0 \leq n < R \\ X_{data}[n] & \text{for } R \leq n < N \end{cases} \quad (11)$$

where the values of  $X_{SI}$  are optimised and may be grouped, and  $R = N - P$ . Finally, (10) can be rewritten as

$$\tilde{x}_{tx} = \sum_{v=1}^V \tilde{b}^v \cdot \text{IDWPT}\{X_{tx}^v\} \quad (12)$$

Fig. 4 shows the proposed reconstruction scheme of the original signal. The signal  $r$  is the received data and the original data  $\tilde{X}$  are obtained after the DWPT operation. Then, the first  $R$  data are

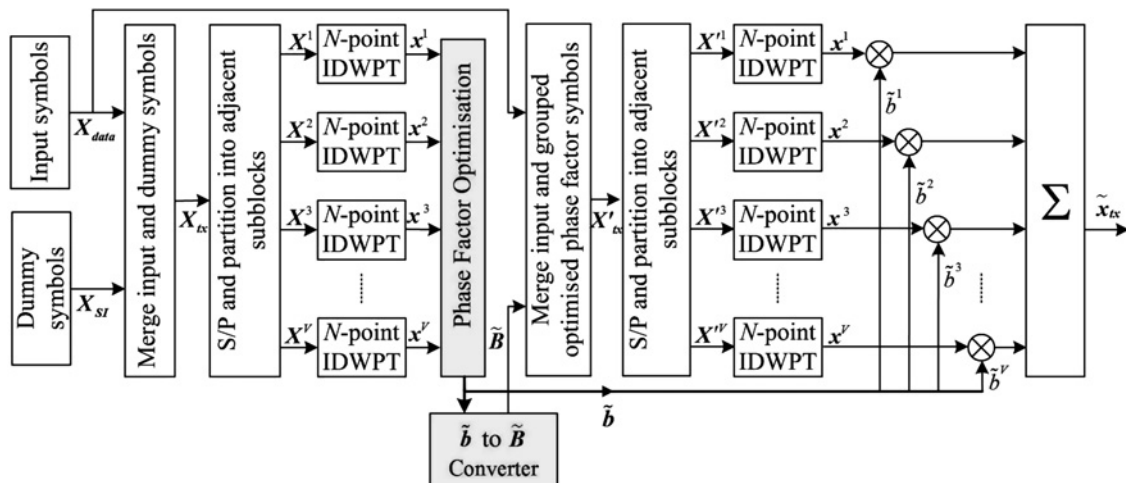


**Fig. 2** Proposed WP-PTS-ESID scheme

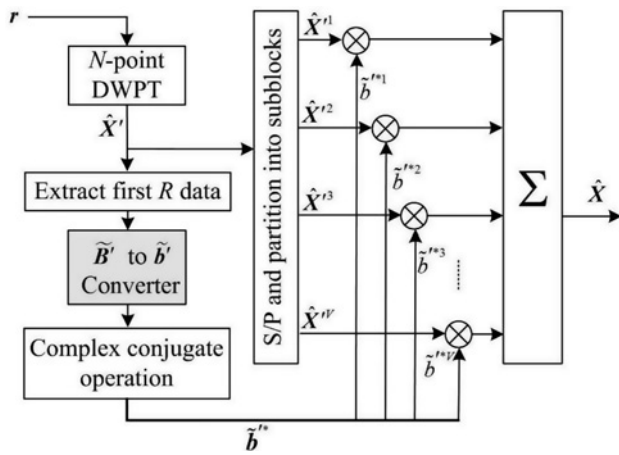


Fig. 4 Proposed reconstruction of WP-PTS-ESID scheme

extracted from  $\hat{X}'$  and labelled as

$$\hat{X}'_{SI}[n] = \tilde{B}'_n \quad \text{for } 0 \leq n < R \quad (13)$$

$\tilde{B}'$  can be an individual or group of several  $\tilde{b}'$ s; hence, the block of ' $\tilde{B}'$  to  $\tilde{b}'$  converter' is utilised to generate the  $\tilde{b}'$  sequence by applying the complex conjugate operation. This block is further elaborated in Section 3.3. The complex conjugate of  $\tilde{b}'$  elements can be described as

$$\tilde{b}'^* = [\tilde{b}'^{*1}, \tilde{b}'^{*2}, \dots, \tilde{b}'^{*V}] \quad (14)$$

Finally,  $\hat{X}'$  data sequence is also divided evenly into  $V$  disjoint adjacent subblocks and multiplied with  $\tilde{b}'^*$ . The recovered information  $\hat{X}$  is expressed as

$$\hat{X} = \sum_{v=1}^V \tilde{b}'^{*v} \cdot \hat{X}'^v \quad (15)$$

### 3.2 Data structure

As shown previously in Fig. 3, the data frame structure of the input is formed by concatenating  $R$  symbols (of SI data) and  $P$  symbols (of the original data). We set the length of codeword  $R$  to 1/16 of the length of the  $N$  codeword for the simple division of the data frame.

Another important parameter is the total number of disjoint adjacent subblock  $V$ . The number of phase factors consumed must also be the same as the number of  $V$ . In this study, we allocate any number of multiple  $2^j$  of the optimised phase factor elements to a fixed length of the  $R$  codeword, where  $j \forall$  is a positive integer number. Hence, we define three cases as follows:

- (i) Case I – total number of disjoint subblocks  $V$  is less than or equal to the length of the SI data codeword  $R$ , i.e.  $V \leq R$
- (ii) Case II – total number of disjoint subblocks  $V$  is twice the length of the SI data codeword  $R$ , i.e.  $V = 2R$
- (iii) Case III – total number of disjoint subblocks  $V$  is four times the length of the SI data codeword  $R$ , i.e.  $V = 4R$

Fig. 5 illustrates the frame division and SI data element according to their cases. In case I, each phase factor is represented by a single SI data. However, in cases II and III, multiple phase factors are combined. Table 2 shows the relationship of parameters  $N$ ,  $R$ , and  $V$ , and their various cases.

Another important parameter in this work is the number of phase factors that can be selected  $w$ .  $w = 2$  or  $4$  are chosen for the simple

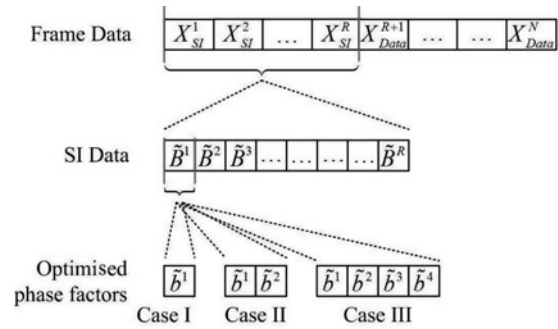


Fig. 5 Frame division and the element of SI data according to the cases

analysis. In Table 3, the possible value for the phase factor to be chosen during the optimisation process with respect to  $w$  is tabulated.

### 3.3 Proposed algorithms

The proposed scheme has two algorithmic blocks: PFO and ' $\tilde{b}'$  to  $\tilde{B}'$  converter'. ' $\tilde{B}'$  to  $\tilde{b}'$  converter' is also developed while at the receiver.

**3.3.1 Algorithm 1: PFO:** This algorithm aims to find the most appropriate phase factor  $\tilde{b}$  for each disjoint subblock to produce the lowest PAPR value. The optimised phase factor sequence is denoted as  $\tilde{b}$ . The parameters of  $V$  and  $w$  must be defined before operation begins.

From Algorithm 1 (see Fig. 6), the term  $v$  is used as a counter for parameter  $V$ , where  $v$  is the current disjoint subblock. The term  $m$  is used as a counter for parameter  $w$ , where  $m$  is the integer that associates the possible value of a phase factor shown in Table 3. If  $w = 4$  is chosen, then the counter of  $m$  has the component  $m = \{1, 2, 3, 4\}$ ; hence, the corresponding phase factor  $b$  is  $b = \{1, j, -1, -j\}$ . Moreover, the terms  $b_{\text{before}}$ , PAPR $_m$ , and PAPR $_{\text{min}}$  in this algorithm are considered memory elements.

Table 2 Relationships between  $N$ ,  $R$ ,  $V$ , and cases

$N$	$R$	$V$	Case type
64	4	1	I
		2	I
		4	I
		8	II
		16	III
		32	n/a
128	8	64	n/a
		1	I
		2	I
		4	I
		8	I
		16	II
256	16	32	III
		64	n/a
		1	I
		2	I
		4	I
		8	I
		16	I
		32	II
		64	III
		1	I
		2	I
		4	I

Table 3 Possible value for phase factor,  $b$

Number of phase factor, $w$	Phase factor, $b$
2	$1, -1$
4	$1, j, -1, -j$

---

**Algorithm 1**


---

**Require:**  $V, w$  and  $\mathbf{X}_{\text{tx}}$ 
**Ensure:**  $\tilde{\mathbf{b}}^v = [\tilde{b}^1, \tilde{b}^2, \tilde{b}^3, \dots, \tilde{b}^V]$ 

```

1:  $v \leftarrow 1$ 
2:  $m \leftarrow 1$ 
3:  $\mathbf{x}_{\text{tx}} = \sum_{v=1}^V b^v \cdot \text{IDWPT} \{ \mathbf{X}_{\text{tx}}^v \}$ 
4:  $\text{PAPR}m \leftarrow \text{PAPR}(\mathbf{x}_{\text{tx}})$  {Calculate initial PAPR}
5: if  $v = 1$  then
6:    $\text{PAPR}min \leftarrow \text{PAPR}m$ 
7:    $v \leftarrow v + 1$ 
8: end if
9: for  $v = 2$  to  $V$  do
10:  for  $m = 1$  to  $w$  do
11:    $b_{\text{before}} \leftarrow b^v$  { $b^v$  is copied from  $\mathbf{b}$  sequence element of order  $v$ }
12:    $b^v \leftarrow b^m$ 
13:    $\mathbf{x}_{\text{tx,new}} = \sum_{v=1}^V b^v \cdot \text{IDWPT} \{ \mathbf{X}_{\text{tx}}^v \}$ 
14:    $\text{PAPR}m \leftarrow \text{PAPR}(\mathbf{x}_{\text{tx,new}})$ 
15:   if  $\text{PAPR}m < \text{PAPR}min$  then
16:      $\text{PAPR}min \leftarrow \text{PAPR}m$ 
17:   else
18:      $b^v \leftarrow b_{\text{before}}$ 
19:   end if
20:  end for
21: end for
22: for  $v = 1$  to  $V$  do
23:   $\tilde{b}^v \leftarrow b^v$ 
24: end for

```

---

**Fig. 6** Phase factor optimisation

The function to compute PAPR for the current data frame is indicated as  $\text{PAPR}\{\cdot\}$ . Finally, this algorithm produces the optimised phase factor sequence, which is denoted as  $\tilde{\mathbf{b}}$ .

**3.3.2 Algorithm 2:  $\tilde{\mathbf{b}}$  to  $\tilde{\mathbf{B}}$  converter:** This block receives the optimised phase factor elements  $\tilde{b}$  in multiples of  $2^l$  integers and converts them into  $R$  elements of SI data. For this purpose, the parameters  $N$  and  $V$ , as well as the case type, must be identified by referring to Table 2.

For example, during the optimisation process when  $w = 4$ , the element in the  $\tilde{\mathbf{b}}$  sequence consists of  $\{1, j, -1, -j\}$ . We have to manipulate these elements into an integer factor (i.e. symbol with upper dot) as represented in Table 4.

To generate SI data,  $\tilde{\mathbf{B}}$  sequence, we then introduce the SI integer,  $M_B$ . The relationships between the integer factor (i.e.  $\dot{b}$ ) and the SI integer (i.e.  $M_B$ ) is in accordance with the case type as follows:

Case 1:  $V \leq R$

$$M_B = \dot{b} \quad (16)$$

Case 2:  $V = 2R$

$$M_B = \dot{b}^1 \times w^1 + \dot{b}^2 \times w^0 \quad (17)$$

Case 3:  $V = 4R$

$$M_B = \dot{b}^1 \times w^3 + \dot{b}^2 \times w^2 + \dot{b}^3 \times w^1 + \dot{b}^4 \times w^0 \quad (18)$$

**Table 4** Current phase factor to integer factor conversion

Optimised phase factor, $\tilde{b}$	Integer factor, $\dot{b}$
1	0
-1	1
$j$	2
$-j$	3

where  $\dot{b}^k$  is the integer factor ( $k$  is the order within the current group of the data frame), whereas  $w^n$  is the corresponding number of allowable phase factors to the power of  $n$ .

To calculate SI data  $\tilde{\mathbf{B}}$ , two parameters are required: the SI integer, i.e.  $M_B$ , and the maximum value of the SI integer, i.e.  $\max(M_B)$ . The SI data  $\tilde{\mathbf{B}}$  can be calculated as follows

$$\tilde{B} = \cos\left(\frac{M_B}{\max(M_B) + 1} \times 2\pi\right) + j \sin\left(\frac{M_B}{\max(M_B) + 1} \times 2\pi\right) \quad (19)$$

The value of  $\max(M_B)$  can be determined according to case type. We use the number of phase factor  $w = 2$  throughout the result estimation. Table 5 shows the important parameters and the value of  $\max(M_B)$ . The calculation of  $\max(M_B)$  is based on (16)–(18) when the maximum value of base 2 is considered.

**3.3.3 Algorithm 3:  $\tilde{\mathbf{B}}$  to  $\tilde{\mathbf{b}}'$  converter:** SI data have  $R$  components extracted from the received data frame  $\tilde{\mathbf{X}}'$  (Fig. 4). This block reproduces  $V$  phase factors for data reconstruction. Thus, each  $\tilde{B}$  symbol can be rewritten to follow (19) as

$$\tilde{B}' = \cos\left(\frac{M_B'}{\max(M_B') + 1} \times 2\pi\right) + j \sin\left(\frac{M_B'}{\max(M_B') + 1} \times 2\pi\right) \quad (20)$$

**Table 5** Integer factor with maximum value

Case	Integer factor codeword	Max. value of base $w$ ( $w = 2$ )	$\max(M_B)$
I	$\dot{b}$	1	1
II	$\dot{b}^1 \dot{b}^2$	11	3
III	$\dot{b}^1 \dot{b}^2 \dot{b}^3 \dot{b}^4$	1111	15

### Algorithm 2

**Require:**  $M_{B1}'$ ,  $M_{B2}'$  and  $\max(M_{B1}')$

**Ensure:**  $M_B'$

- 1:  $sign = M_{B2}' / |M_{B2}'|$
- 2: **if** ( $sign = 0$  **or**  $sign \geq 0$ ) **then**
- 3:  $M_B' \leftarrow M_{B1}'$
- 4: **else if** ( $sign \leq 0$ ) **then**
- 5:  $M_B' \leftarrow \max(M_{B1}') + 1 - M_{B1}'$
- 6: **end if**

**Fig. 7** To obtain the exact  $M_B'$

where the prime notation indicates that the parameters are at the receiver part, i.e.  $M_B'$  is equivalent to  $M_B$  (similar to that in the transmitter). Hence, for each element of  $\tilde{B}'$  symbol, two different representations for the term  $M_B'$  (labelled as  $M_{B1}'$  and  $M_{B2}'$ ) are obtained as follows

$$M_{B1}' = \cos^{-1}(\tilde{B}'_{\text{real}}) \cdot \frac{\max(M_B') + 1}{2\pi} \quad (21a)$$

$$M_{B2}' = \sin^{-1}(\tilde{B}'_{\text{imag}}) \cdot \frac{\max(M_B') + 1}{2\pi} \quad (21b)$$

where  $\tilde{B}'_{\text{real}}$  is the real part of  $\tilde{B}'$  and  $\tilde{B}'_{\text{imag}}$  is its imaginary part. We can obtain  $M_B'$  accurately using Algorithm 2 (see Fig. 7). Then, the received integer factors  $b'$  can be determined by manipulating  $M_B'$  according to the following:

Case 1:  $V \leq R$

$$b' = M_B' \quad (22)$$

Case 2:  $V = 2R$

$$b'^1 = \lfloor M_B' / w^1 \rfloor \quad (23a)$$

$$b'^2 = M_B' \bmod w^1 \quad (23b)$$

Case 3:  $V = 4R$

$$b'^1 = \lfloor M_B' / w^3 \rfloor \quad (24a)$$

$$b'^2 = \left\lfloor \frac{M_B' - b'^1 \times w^3}{w^2} \right\rfloor \quad (24b)$$

$$b'^3 = \left\lfloor \frac{M_B' - b'^1 \times w^3 - b'^2 \times w^2}{w^1} \right\rfloor \quad (24c)$$

$$b'^4 = (M_B' - b'^1 \times w^3 - b'^2 \times w^2) \bmod w^1 \quad (24d)$$

where  $w^n$  is the corresponding number of the allowable phase factors to the power of  $n$ ,  $\lfloor \cdot \rfloor$  is the floor bracket, and  $a \bmod b$  gives the remainder from the division of  $a$  by  $b$ .

Finally, we change each of the received integer factor to the received phase factor elements to recover the information on the next operation of complex conjugate based on Table 6.

**Table 6** Received integer factor to received phase factor conversion

Received integer factor, $b'$	Received phase factor, $\tilde{b}'$
0	1
1	-1
2	$j$
3	$-j$

**Table 7** Simulation parameters

Set	Uncoded WP-OFDM	Proposed scheme	Related work
1	$N = 256$ , 16-QAM	$N = 256$ , 16-QAM $V = 4, 8$	$N = 256$ , 16-QAM
2	$N = 64$ , 64-QAM	$N = 64$ , 64-QAM $V = 8, 16$	PRC $V = 4, 8$ [17] $N = 64$ , 64-QAM
3	$N = 64$ , 16-QAM	$N = 64$ , 16-QAM $V = 8, 16$	91-HEX $V = 8, 16$ [20] $N = 64$ , 16-QAM tree pruning with SI 3,6-bits [6]

## 4 Results and discussion

The proposed WP-PTS-ESID scheme is simulated to analyse and compare its performance with two other renowned works, namely, the non-explicit SI [17] and the modified constellation [20], which have been discussed in Section 1. We observe the trade-off between PAPR reduction and BER performance. Moreover, we investigate how much PAPR reduction can be achieved through the proposed scheme by comparing its result with the work of [6] which is mainly a WP tree pruning method. The parameters of the simulation execution are organised in Table 7. The parameters of  $N = 64, 128$  and 16-QAM, 64-QAM modulations are widely used in 802.11 standards [31]. Therefore, the choice for the mentioned parameters makes the proposed work feasible for practical application.

A major practical drawback found in the MCM transmission method such as the conventional OFDM system is the yield of random envelopes with high peak. When the high peak signal operates in the non-linear region of the power amplifier at the transmitter, the system experiences non-linear distortion [15]. The PTS related works introduced in [17, 20] effectively reduce the high PAPR with the expense of acceptable BER performance degradation. However, their methods ignore the SI data. In this work, we consider the trade-off between deteriorating the PAPR (to an acceptable limit) by adding the SI data to the frame at the transmitter and the improvement of the BER performance. Therefore, this serves as the motivation for obtaining the results of the proposed scheme.

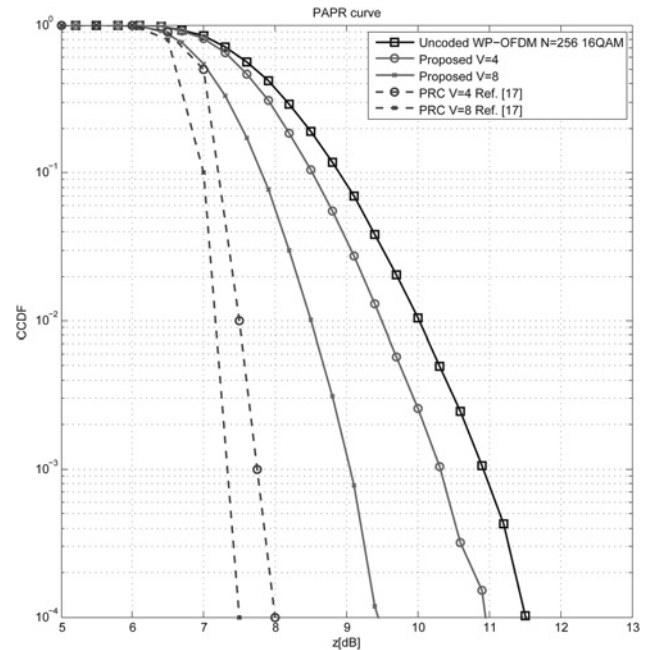


**Fig. 8** CCDF of PAPR for the proposed WP-PTS-ESID scheme compared with the PRC scheme [17], for  $V = 4$  and  $8$

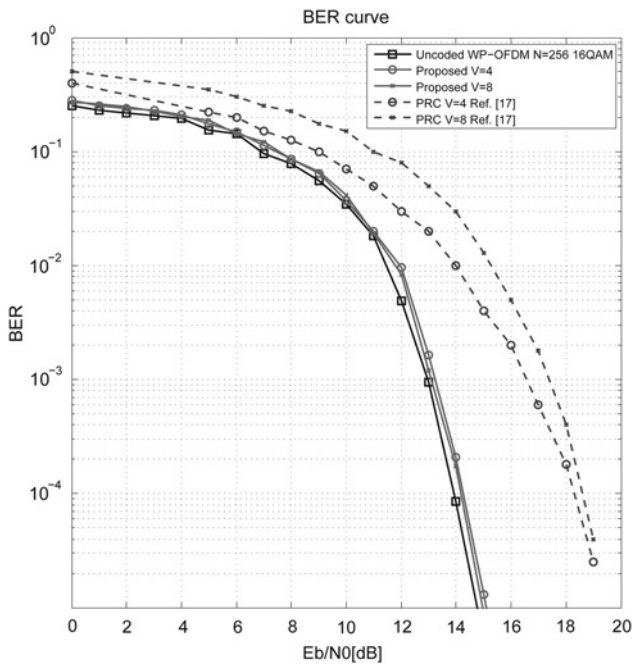


**Fig. 9** BER performance of the proposed WP-PTS-ESID scheme, compared with the PRC scheme [17], for  $V = 4$  and  $8$

The CCDF of the PAPR is utilised to evaluate the performance and is defined as follows

$$\text{CCDF}(\text{PAPR}(x[n])) = \Pr(\text{PAPR}(x[n]) > \text{PAPR}_0)$$

where  $\text{PAPR}_0$  is a certain threshold value that is typically given in decibels relative to the root mean square value.

*Set 1:* Fig. 8 shows the CCDFs of the PAPR for the proposed WP-PTS-ESID scheme compared with that of the first approach, i.e. non-explicit SI. The original uncoded WP-OFDM system, which exhibits no PAPR reduction, is also included. The result

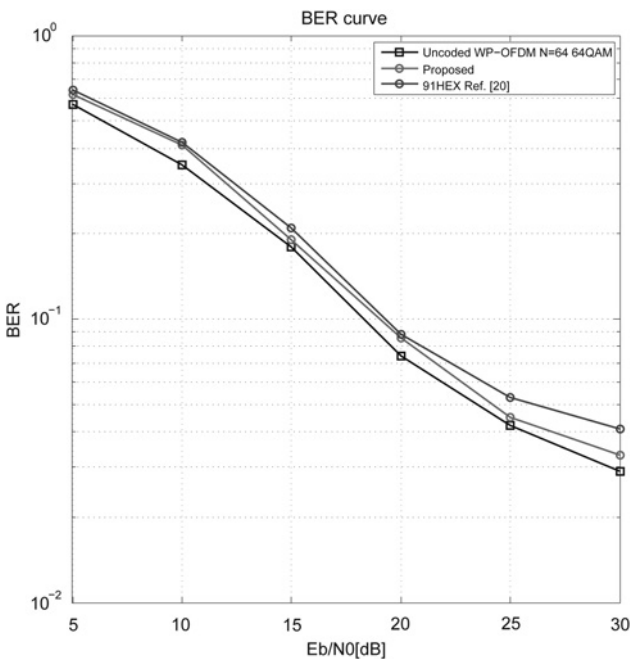


**Fig. 11** BER performance of the proposed WP-PTS-ESID scheme compared with 91-HEX [20] under a Rayleigh fading channel

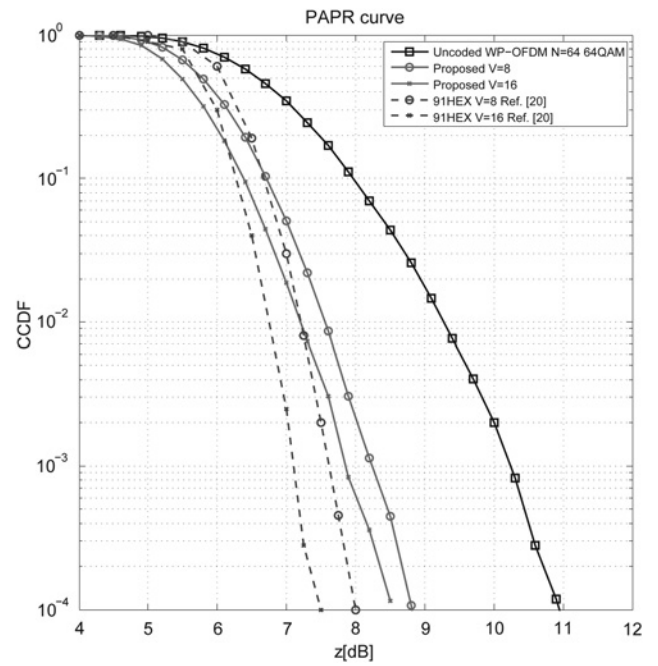


**Fig. 10** CCDF of PAPR for the proposed WP-PTS-ESID scheme compared with scheme represented as 91-HEX [20],  $V = 8$  and  $16$

shows that for similar parameters of  $V = 8$  at a CCDF of  $10^{-4}$ , the proposed scheme can achieve a reduction of nearly 2 dB from its uncoded WP-OFDM, whereas the PRC scheme achieves 4 dB. However, the PRC scheme suffers from BER degradation, and thus, an additional 4 dB is required, compared with that of the proposed scheme at a similar BER level of  $10^{-4}$  as shown in Fig. 9. *Set 2:* Fig. 10 shows the CCDFs of the PAPR for the proposed WP-PTS-ESID scheme compared with the second approach, i.e. modified constellation by including the original uncoded WP-OFDM system without PAPR reduction. Under the same parameter of  $V = 16$  at a CCDF of  $10^{-3}$ , the proposed scheme

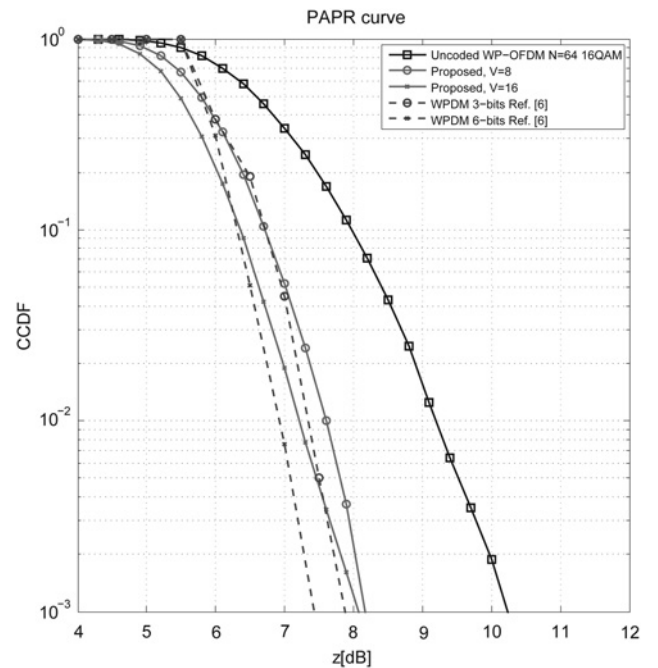


**Fig. 12** CCDF of PAPR for the proposed WP-PTS-ESID scheme and the related work of WP tree pruning scheme [6] with corresponding  $I = 4, 6$  bits, respectively

**Table 8** Comparison in terms of the frame length for the proposed scheme and other works [6, 9]

Selected $N$	Proposed ( $N$ )	Other related work ( $N$ )	Overhead
64	60 data + 4 SI	64 [6]	$\frac{4SI}{64} = \frac{1}{16}$
128	120 data + 8 SI	128 [9]	$\frac{8SI}{128} = \frac{1}{16}$

achieves a reduction of nearly 2.5 dB, whereas the compared 91-HEX scheme exhibits a slight improvement of 3 dB. The proposed scheme with  $V = 16$  selection demonstrates considerably better BER performance under the Rayleigh fading channel as shown in Fig. 11.

*Set 3:* Fig. 12 shows the CCDFs of the PAPR for the proposed WP-PTS-ESID scheme compared with the other WP-based scheme, i.e. WP tree pruning [6]. In particular, each alternative tree results in a different value for the PAPR; hence, the algorithm is used to achieve minimum PAPR. However, this method produces SI. We select two examples from the aforementioned literature where SI carries 3 bits and 6 bits of data. As shown in the figure, we can verify that the proposed scheme can reduce the PAPR of the signals as compared with the uncoded WP-OFDM and relatively at the same performance with the WP tree pruning scheme [6] at low dB.

Table 8 shows the comparison of the frame length for the proposed scheme and other related works [6, 9]. The table indicates that the proposed scheme always has 1/16 of the entire frame overhead induced as compared with other related works [6, 9] where no SI data added.

Furthermore, the BER performance of the proposed WP-PTS-ESID scheme is compared with the WP tree pruning scheme [6]. In that work, when the SI  $I = 6$  bits, this requires two of the 16-QAM symbols to be sacrificed [i.e. two out of 64 available total subcarriers (frame length)]. This results a frame with a code rate of 62/64. Since the proposed WP-PTS-ESID scheme has the code rate of 60/64, in order to have a fair performance comparison we match the code rates using rate matching operation to be  $(60/64) \times (62/60) = 62/64$ . Fig. 13

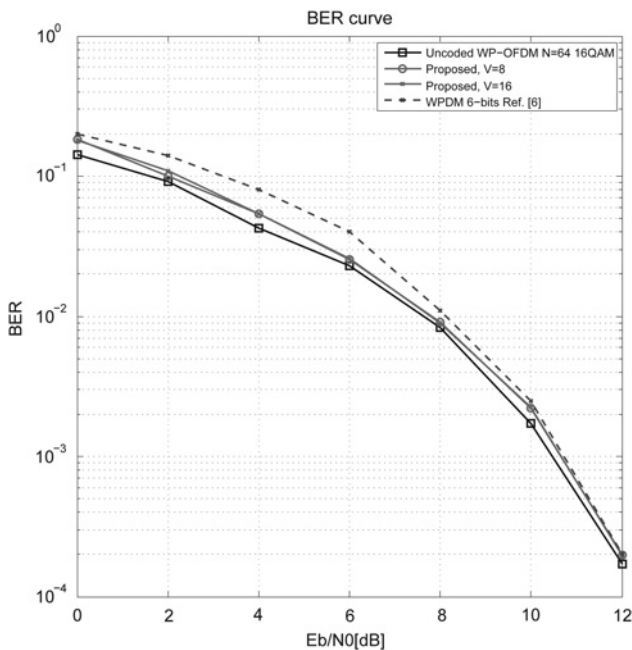


**Fig. 13** BER performance comparison between the proposed WP-PTS-ESID scheme and the related work of wavelet packet tree pruning scheme [6] with corresponding  $I = 6$  bits

shows the BER performance comparison where the proposed WP-PTS-ESID scheme outperforms the work in [6] at low to medium energy per bit to noise ratio ( $E_b/N_0$ ) values.

## 5 Conclusion

In this study, a new PAPR reduction technique known as the WP-PTS-ESID scheme is proposed. This scheme embeds SI data into the data frame. The simulation results show that the proposed WP-PTS-ESID scheme can achieve PAPR reduction that is similar to those of renowned works. The BER increase of the proposed scheme is typically insignificant compared with the uncoded original signals, and its BER performance is considerably better than those of other renowned schemes.

## 6 Acknowledgment

The authors thank University of Science Malaysia Research University Post Graduate Research Scheme grant for supporting this research under grant no. 1001/PELECT/814178.

## 7 References

- Jamin, A., Mähönen, P.: 'Wavelet packet modulation for wireless communications: research articles', *Wirel. Commun. Mob. Comput.*, 2005, 5, (2), pp. 123–137
- Kumbasar, V., Kucur, O.: 'Performance comparison of wavelet based and conventional OFDM systems in multipath Rayleigh fading channels', *Digit. Signal Process.*, 2012, 22, (5), pp. 841–846
- Okamoto, E., Iwanami, Y., Ikegami, T.: 'Multimode transmission using wavelet packet modulation and OFDM'. IEEE Conf. Vehicular Technology, 2003
- Daoud, O.: 'Performance improvement of wavelet packet transform over fast Fourier transform in multiple-input multiple-output orthogonal frequency division multiplexing systems', *IET Commun.*, 2012, 6, (7), pp. 765–773
- Han, S.H., Lee, J.H.: 'An overview of peak-to-average power ratio reduction techniques for multicarrier transmission', *IEEE Wirel. Commun.*, 2005, 12, (2), pp. 56–65
- Baro, M., Ilow, J.: 'PAPR reduction in wavelet packet modulation using tree pruning'. IEEE Vehicular Technology Conf., 2007, pp. 1756–1760
- Jiao-Jun, L., Heng, L., Li-Yun, S.: 'Fast adaptive optimal basis search algorithm for PAPR reduction'. IEEE Int. Conf. on Computer Science and Automation Engineering (CSAE), 2011
- Patel, V.V., Patil, R.N.: 'Minimization of PAPR in OFDM system using IDWT/DWT, clipping and filtering combined with Huffman coding method'. Int. Conf. on Communications and Signal Processing (ICCCSP), 2013
- Lixia, M., Murrioni, M.: 'Peak-to-average power ratio reduction in multi-carrier system using genetic algorithms', *IET Signal Process.*, 2011, 5, (3), pp. 356–363
- Dixit, N., Singh, N., Mandake, S., et al.: 'A genetic algorithm based PAPR reduction in WPM system'. Tenth Int. Conf. on Wireless and Optical Communications Networks (WOCN), 2013
- Rostamzadeh, M., Vakily, V.T.: 'PAPR reduction in wavelet packet modulation'. 5th Int. Multi-Conf. on Systems, Signals and Devices, IEEE SSD 2008, 2008
- Huang, X., Tan, G., Xu, Q., et al.: 'A kind of PAPR reduction method based on pruning WPM and PTS technology', *J. Electron.*, 2013, 30, (3), pp. 261–267
- Li, L., Qu, D.: 'Joint decoding of LDPC code and phase factors for OFDM systems with PTS PAPR reduction', *IEEE Trans. Veh. Technol.*, 2013, 62, (1), pp. 444–449
- Li, L., Qu, D., Jiang, T.: 'Partition optimization in LDPC-coded OFDM systems with PTS PAPR reduction', *IEEE Trans. Veh. Technol.*, 2014, 63, (8), pp. 4108–4113
- Rahmatallah, Y., Mohan, S.: 'Peak-to-average power ratio reduction in OFDM systems: a survey and taxonomy', *IEEE Commun. Surv. Tutor.*, 2013, 15, (4), pp. 1567–1592
- Zakaria, J., Salleh, M.F.M.: 'On the PAPR reduction technique: WP-PTS scheme with embedding the side information data'. IEEE 11th Malaysia Int. Conf. on Communications (MICC 2013) – Mobile and Wireless Communications 2013, 2013
- Yang, L., Soo, K.K., Li, S.Q., et al.: 'PAPR reduction using low complexity PTS to construct of OFDM signals without side information', *IEEE Trans. Broadcast.*, 2011, 57, (2), pp. 284–290
- Kim, H., Hong, E., Ahn, C., et al.: 'A pilot symbol pattern enabling data recovery without side information in PTS-based OFDM systems', *IEEE Trans. Broadcast.*, 2011, 57, (2), pp. 307–312
- Eom, S.-S., Nam, H., Ko, Y.-C.: 'Low-complexity PAPR reduction scheme without side information for OFDM systems', *IEEE Trans. Signal Process.*, 2012, 60, (7), pp. 3657–3669
- Han, S.H., Cioffi, J.M., Lee, J.H.: 'On the use of hexagonal constellation for peak-to-average power ratio reduction of an OFDM signal', *IEEE Trans. Wirel. Commun.*, 2008, 7, (3), pp. 781–786
- Li, C., Jiang, T., Zhou, Y., et al.: 'A novel constellation reshaping method for PAPR reduction of OFDM signals', *IEEE Trans. Signal Process.*, 2011, 59, (6), pp. 2710–2719

- 22 Liang, H.: 'Combining block-coded modulation codes and improved constellation extended schemes to reduce peak-to-average power ratio in orthogonal frequency-division multiplexing systems', *IET Commun.*, 2012, **6**, (16), pp. 2705–2714
- 23 Pighi, R., Raheli, R.: 'Joint decoding of TCM and detection of PTS side information: a multiple trellis solution'. IEEE Int. Symp. on Power Line Communications and its Applications, 2007
- 24 Tan, G., Li, Z., Su, J., *et al.*: 'Superimposed training for PTS-PAPR reduction in OFDM: a side information free data recovery scheme'. Eighth Int. ICST Conf. on Communications and Networking in China (CHINACOM), August 2013, pp. 694–698
- 25 Ku, S.-J., Wang, C.-L.: 'A new side-information free PTS scheme for PAPR reduction in OFDM systems'. IEEE 8th Int. Conf. on Wireless and Mobile Computing, Networking and Communications (WiMob), October 2007, pp. 108–112
- 26 Lim, D.-W., Heo, S.-J., No, J.-S.: 'An overview of peak-to-average power ratio reduction schemes for OFDM signals', *J. Commun. Netw.*, 2009, **11**, (3), pp. 229–239
- 27 Henkel, W., Taubock, G., Ödler, P., *et al.*: 'The cyclic prefix of OFDM/DMT – an analysis'. Int. Zurich Seminar on Broadband Communications, 2002. Access, Transmission, Networking, 2002
- 28 Muller, S.H., Huber, J.B.: 'OFDM with reduced peak-to-average power ratio by optimum combination of partial transmit sequences', *Electron. Lett.*, 1997, **33**, pp. 368–369
- 29 Muller, S.H., Huber, J.B.: 'A comparison of peak power reduction schemes for OFDM'. IEEE Global Telecommunications Conf., 1997
- 30 Muller, S.H., Huber, J.B.: 'A novel peak power reduction scheme for OFDM'. The 8th IEEE Int. Symp. on Personal, Indoor and Mobile Radio Communications, 1997
- 31 Geier, J.T.: 'Designing and deploying 802.11n wireless networks' (Cisco Press, 2010)